

Article

Strength Development and Environmental Assessment of Full Tailings Filling Materials with Various Water-to-Binder Ratios

Zhu Ding ^{1,2} , Pai Liu ³, Peng Cui ^{1,2,*} and Chengyu Hong ^{1,2} ¹ College of Civil and Transportation Engineering, Shenzhen University, Shenzhen 518060, China² Guangdong Province Key Laboratory of Durability for Marine Civil Engineering, Shenzhen 518060, China³ Gd Midea Air-Conditioning Equipment Co., Ltd., Foshan 528312, China

* Correspondence: 2150471024@email.szu.edu.cn

Abstract: In order to build green mines, goaf is often filled, supported, and sealed with a high-water material to eliminate a series of environmental problems and safety hazards caused by goaf. In this study, ordinary Portland cement, sulphoaluminate cement, and alkali-activated cement were used as binders to prepare full-tailings high-water materials for filling, with various water-to-cement ratios. The compressive strength development of consolidated tungsten tailings specimens prepared with various curing binders was observed, and the influence of various water–cement ratios on the strength development was analyzed. The environmental impact of mine backfill materials was assessed according to the life cycle theory (LCA), and these mine backfill materials were prepared by using various binders. The results show that when the water-to-binder ratio is 3, the strength of alkali-activated cement can reach 3 MPa at 28 days; at that ratio, the microstructure of alkali-activated cement is more compact. Through LCA analysis, the environmental load of alkali-activated cement is shown to be significantly lower than that of either Portland cement or sulphoaluminate cement; the LCA results show that the primary energy consumption using alkali-activated cement is reduced from the Portland and sulphoaluminate cements by 1319.32 MJ and 945 kg, respectively. These unusual reduction percentages are achieved because the production of alkali-activated cement by LCA does not have any negative environmental impact—the production of alkali-activated cement, with its primary component being industrial byproduct slag, so that the use of alkali-activated cement in tailings’ consolidation has a positive environmental impact.



Citation: Ding, Z.; Liu, P.; Cui, P.; Hong, C. Strength Development and Environmental Assessment of Full Tailings Filling Materials with Various Water-to-Binder Ratios. *Metals* **2023**, *13*, 122. <https://doi.org/10.3390/met13010122>

Academic Editor: Antoni Roca

Received: 18 September 2022

Revised: 11 December 2022

Accepted: 27 December 2022

Published: 7 January 2023



Copyright: © 2023 by the authors. Licensee MDPI, Basel, Switzerland. This article is an open access article distributed under the terms and conditions of the Creative Commons Attribution (CC BY) license (<https://creativecommons.org/licenses/by/4.0/>).

Keywords: tungsten tailings; alkali-activated cement; environmental benefits; economic performance; mine filling; full tailings filling

1. Introduction

There are many environmental pollution mechanisms through which society mistreats the environment, but solid waste is the most significant. Solid waste accumulation can seriously work against the sustainable development of society, so achieving large-scale solid waste resource utilization has become an urgent problem. After the extraction of mineral resources, a large amount of mine solid waste will remain, including waste rock, tailings, and gangue. Mining creates large volumes of these wastes, which are difficult to reuse. The traditional treatment method is mainly stacking, and now the tailings have exceeded 5 billion tons, and this number is still increasing [1–3] in the world. Moreover, the chemical compositions of mine tailings range from 60% to 90% and are mainly silicon, aluminum, and calcium oxides [2]. The overall utilization rate of these tailings in China is relatively low, i.e., less than 11% [4]. At present, green mine construction and tailings resource treatment is one of the key points to help the construction of the zero-waste city in China.

In mining operations, the cavity is called goaf after removing the ore-bearing material. The existence of goaf brings a series of environmental problems and security risks, such as

surface subsidence or even collapse, putting people in danger of falls into the goaf, and so on [5]. These concerns call for proper treatment and protection methods in the mined area. The conventional treatment methods are primarily caving surrounding rock, filling, supporting, and closing the mined area.

About 62.1% of the global tungsten resource reserves are located in China, and 90.9% of tungsten products produced come from China [6,7]. There are five major tungsten metallogenic belts in China, namely in North China, South China, Mountain Tian and Mountain Bei, West Qinling Mountain Qilian, and the Three Rivers metallogenic belts, but more than 70% of the tungsten reserve is in South China [8,9]. For the hydrometallurgical process of the tungsten ore, more than 50% of the particle size of the tungsten mailing is less than 10 μm [10–12]. Therefore, the tungsten mailing can be used as a commercial raw material for inert glass–ceramic [11–13]. In addition, some researchers used the activated tungsten mailing instead of cement clinker to deal with the tailings pollution and reduce cost for cement materials [14]. The tungsten mailing also can be used as a raw material for preparing ceramic substrate [15,16]. Tungsten mine-waste-mud geopolymeric binder was studied to develop a new binder for mineral-waste mud [17,18].

Filling is the main way to deal with the mine solid waste. In the 1980s, the high-water packing material (i.e., water-to-cementing-binder ratio greater than 0.65) had been used as paste backfill material. For the underground industrial experiment, the paste backfill material was put in a coal mine as a raw material. It was found that the paste backfill material had good stability, and it was easy to control with an economical and environmentally friendly method [19]. Paste backfill material is mainly used as an essential raw material in the fields of rock-stability maintenance, grouting technology, and mine filling because it has some advantages, such as superior fluidity and water fixation capacity, high early strength, and good filling characteristics. Moreover, in order to prepare high early strength, high water content, and quick setting material with good pumpability, bauxite was used as the principal component of the gold tailings cementation materials after the laboratory and engineering application research. Generally, the compressive strength increased with the increasing tailings concentration and the high-water packing material [20,21]. The high-water material was also used to repair port facilities and achieved excellent performances [22]. The freeze–thaw resistance is very important in seasonally frozen regions for the fine-grained soils. However, glass fiber, nano-SiO₂, and the optimal moisture content of tailings can prevent the expansion of the fine-grained soils and improve the mechanical properties under freeze–thaw conditions [23–26].

Life cycle analysis (LCA) is widely used in the various environmental research field [27–30]. LCA is employed in the entire evaluation process, including in the origin of the object, the extinction of the object, and all environmental impacts. With increasing attention being paid to environmental protection, some new material and technology are always applied to realize the sustainable development [30,31]. The LCA theory includes some ex ante LCA studies, and ex ante LCA studies can be used as an environmental screening tool to evaluate research suggestions or design concepts. Furthermore, the ex ante LCA studies are useful for industrial production and can directly improve design and technology to realize the circular economy [31].

In the study reported in this paper, ordinary Portland cement, sulphotoaluminate cement, and alkali-activated cement were used as cementing agents, and various water–solid ratios are used to prepare all tailings high-water materials (as mine backfill). The development of compressive strength of consolidated tungsten tailings is observed, and the influences of various water-to-solid ratios on the compressive strength are analyzed. In addition, the microstructure of the consolidation specimen is studied. At last, some analyses and comparisons are used for the environmental impact assessment based on the life cycle theory.

2. Experimental Procedures and Method of Environmental Assessment

2.1. Raw Materials

The tungsten ore tailings used in this study are from Guangdong Shaogang Jiayang New Material Co., Ltd. (Shaoguan, China). The water content of the original tungsten ore tailings is 70.74%. Because these tailings contain a large amount of water, it will precipitate and cause water sand stratification after standing for a period of time. The precipitated solid part is called the full tailings, while the part with a large amount of water in the upper layer is called the supernatant. In this research, a mixer was used to mix the whole tailings and supernatant before using the tailings. The chemical compositions of the full tailings after drying and of other raw materials were determined by X-ray fluorescence (XRF) spectrometry (S4 EXPLORER, Bruker AXS GmbH, Karlsruhe, Germany). The results are shown in Table 1.

Table 1. Chemical composition of dry tailings and other raw materials by XRF (weight ratio %).

Raw Materials	CaO	SiO ₂	Al ₂ O ₃	MgO	SO ₃	TiO ₂	K ₂ O	Fe ₂ O ₃	MnO	Na ₂ O
Dry tailings	25.03	52.38	6.43	3.17	0.43	0.09	0	11.14	1.12	0.20
Slag	39.99	32.22	15.57	8.78	1.45	0.78	0.35	0.26	0.19	0.42
Anhydrous gypsum	39.48	1.89	0.76	2.00	55.47	0	0.10	0.30	0	0
Quicklime	93.05	5.18	0.54	0.98	0.04	0	0	0.21	0	0

For the dry tailings, there is more than 52% SiO₂ in Table 1. The content of CaO is nearly 40% in the slag and anhydrous gypsum. There is more than 55% SO₃ in the anhydrous gypsum, and there is more than 93% CaO in the quicklime. In addition, the dry tailings are also mainly composed of CaO and Fe₂O₃, with a small amount of Al₂O₃, MgO, MnO, etc. The contained fractions of CaO and Fe₂O₃ are about 25.03% and 11.14%, respectively.

The particle size of dry tailings, slag powder, and limestone powder were measured by an industry-preferred laser diffraction analyzer (Micromeritics S3500, measurement capability from 0.02 to 2800 microns; Seattle, WSU, USA). The results are shown in Figure 1. Figure 1 shows that the particle size distribution of dry tailings is wide, ranging from several microns to several hundred microns. The particle size of slag powder is smaller than that of the limestone powder, and the particle size of limestone powder is smaller than that of the dry tailings in Figure 1. X-ray diffraction (XRD, D8 ADVANCE Bruker, Karlsruhe, Germany) was used for mineral phase analysis of tungsten ore tailings. The results are shown in Figure 2. The XRD analysis shows that there are crystal phase diffraction peaks of SiO₂, CaCO₃, and Ca₃Fe₂(SiO₄)₃ (calcium iron garnet) in the tungsten ore tailings, indicating that the tungsten ore belongs to Skarn-type scheelite tungsten deposit [32,33].

The cementing binders used as filling cementing materials are ordinary Portland cement (P · O 42.5R), high belite sulphoaluminate cement (42.5), and alkali-activated cement. The main raw materials of alkali-activated cement are slag powder, gypsum, limestone powder, quicklime, and sodium sulfate. The GGBF slag powder (S95 grade in the standard of ground granulated blast furnace slag used for cement and concrete (GBT 18046-2008)) was from Guangdong Shaogang Jiayang New Material Co., Ltd. (Shaoguan, China). Sulphoaluminate cement was purchased from Tangshan Polar Bear Building Materials Co., Ltd. (Tangshan, China), with a strength grade of 42.5. The particle size of quicklime is 125 µm; it has a CaO weight ratio of 90%. Anhydrous gypsum with a particle size of 75 µm and calcium–sulfate weight ratio of 99% was used. The weight ratio of anhydrous sodium sulfate in sodium sulfate is 99%. Sulphoaluminate cement, limestone powder, quicklime powder, anhydrous gypsum, and sodium sulfate are all industrial products. The chemical analysis results of various raw materials are shown in Table 1. The mass proportions of the components of alkali-activated cement are 60% slag powder, 15% limestone powder, 1% sodium sulfate, 10% sulphoaluminate cement, 10% anhydrous gypsum, and 4% quicklime powder.

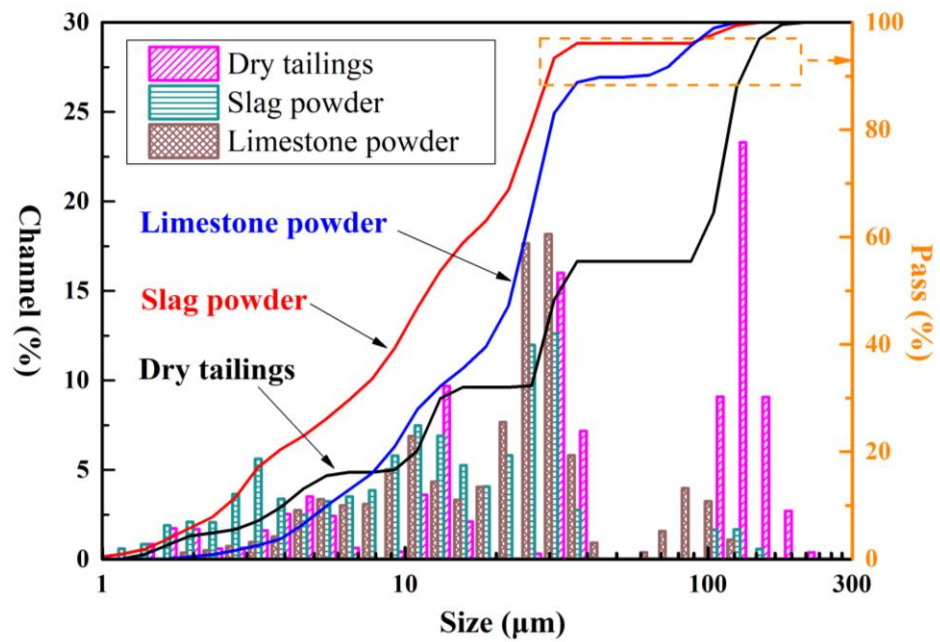


Figure 1. Laser-particle-analysis size-distribution curve of the raw materials.

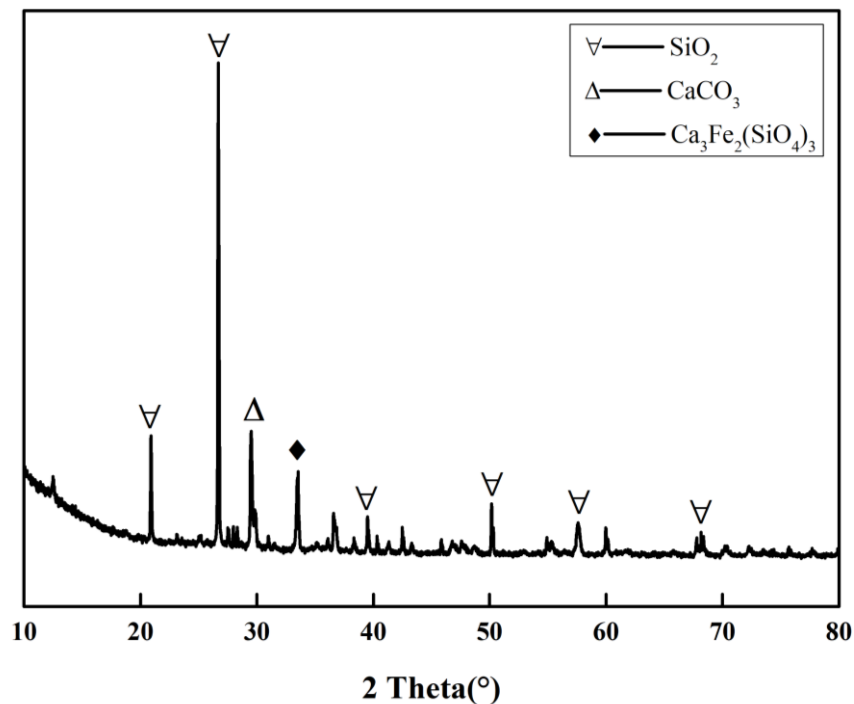


Figure 2. XRD patterns of tungsten ore tailings.

To make the fill cementing material, the tungsten ore tailings and various binders were mixed according to the proportions shown in Table 2. The objective is to compare the effects of using various cementitious materials and various water-to-binder ratios on cured specimens.

2.2. Test Methods

The preparation of the specimen was according to the method for testing the strength of cement mortar (ISO) (GB/T 17671-2021). First, the full tailings (containing water) were mixed evenly, and then the materials were portioned by measured weight according to the

mass converted from the proportion in Table 2 and mixed evenly to form the fresh paste. This fresh paste was poured into the mold (40 mm × 40 mm × 40 mm). The mold filled with fresh paste was put on the cement mortar shaking table and vibrated for 1 min, and then the mold was covered with fresh-keeping film for 3 days in the laboratory air (temperature 20 ± 2 °C, relative humidity $60 \pm 5\%$). After 3 days of drying, the specimens were taken out of the mold and cured in the laboratory's air for 7 days, and these specimens were all tested for compressive strength. Additional specimens, after curing 7 days, were cured in water (temperature 20 ± 1 °C) for 7 days and some for 21 days, and then these specimens were tested for compressive strength, using samples of both the 14 days and 28 days curing durations. All the specimens with a curing age of 7 days (curing in the laboratory's air), 14 days (curing 7 days in the laboratory's air first and then curing 7 days in water), and 28 days (curing 7 days in the laboratory's air first and then curing 21 days in water) were tested for compressive strength, with a loading rate of 0.1 kN/s. The average value of the test results of three specimens of each group is taken as the compressive strength.

Table 2. Material proportions of the tungsten-ore tailings' mixtures.

No.	Binder/Tailings' Weight Ratio	Water/Solid Weight Ratio	Water/Binder Weight Ratio	Binder
A2	0.15	0.34	2	ordinary Portland cement
A3	0.10	0.36	3	
A4	0.07	0.37	4	
B2	0.15	0.34	2	
B3	0.10	0.36	3	high belite sulphoaluminate cement
B4	0.07	0.37	4	
F2	0.15	0.34	2	
F3	0.10	0.36	3	alkali-activated cement
F4	0.07	0.37	4	

After the compressive strength test, some samples were examined for their microstructure characterizations by XRD (with a scanning range of 10–65 degrees and a scan speed of 4 degrees per minute), by scanning electron microscopy (SEM, Quanta FEG 250, FEI Company, Hillsboro, OR, USA), and by mercury intrusion porosimetry technique (MIP, Micromeritics 9620, Micromeritics Instrument Corporation, Norcross, GA, USA).

2.3. Environmental Assessment Methods

The environmental assessment was based on the environmental-management life-cycle-assessment principles and framework (ISO 14040-2006) issued by the International Organization for Standardization. The content of LCA is mainly divided into four parts: target and scope determination, inventory analysis, impact assessment, and result interpretation. These four parts are progressive or repeated, in turn, and run through the input and emission analysis of the entire life cycle process. The specific framework is shown in Figure 3.

After completing these LCA steps, a summary of the previous analysis is made, and a conclusion given to explain the phenomena noted in the previous analysis processes. If there were problems or deficiencies, the probable causes and influencing factors of the situation are documented, and relevant suggestions and opinions are provided within the life cycle assessment, based on the results.

The LCA analysis data in this paper are primarily from eBalance and GaBi software. Currently, eBalance software is the only open database derived by research on domestic life cycle evaluation and analysis in China (Chinese reference life cycle database, developed by Chengdu Yike Environmental Technology Co., Ltd.) (Chengdu, China). In order to facilitate the research work in environmental analysis and environmental protection by

Chinese scholars and enterprises, the database provides over 600 process data sets based on China's production technology and market. It also includes the European basic database ELCD and the Swiss business database convention, and it will be expanded continuously.

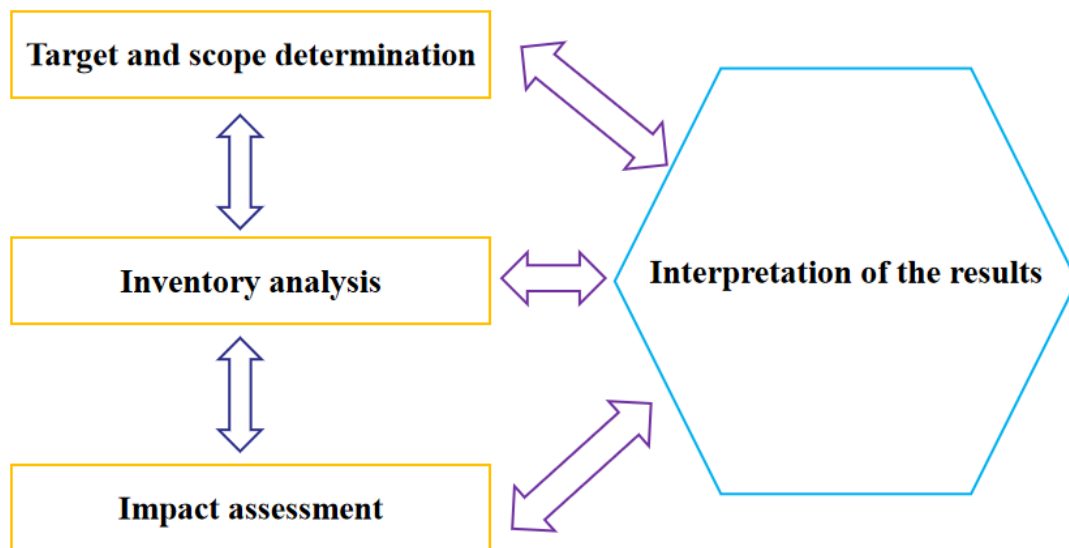


Figure 3. LCA technical framework.

3. Results Analysis and Discussion

3.1. Mechanical Property of Filling Cementitious Material Made of Full Tailings

The mechanical properties, mainly the compressive strength of the materials, are the key factors in practical civil, construction, and mining engineering. Previous determinations are not always definitive because of procedure, precision, instrumentation, variety, comparison, and other factors, including the modern need to consider environmental impact. This study has considered all of these factors in determining the relative merit of three potential goaf-filler materials.

The compressive strengths of the whole tailings-filling cementitious material with three kinds of binders (ordinary Portland cement (A2, A3, and A4), sulphoaluminate cement (B2, B3, and B4), and alkali-activated cement (F2, F3, and F4)) are shown in Figure 4, Figure 5, and Figure 6, for water-to-binder ratios of 2, 3, and 4, respectively.

Figure 4 shows that when the water-to-binder ratio is 2, the compressive strength of all specimens can reach more than 3 MPa, among which the compressive strength of the specimens bonded by sulphoaluminate cement are the highest after curing 7 days. However, the compressive strengths of the specimens bonded by ordinary Portland cement are the lowest and are only about 4 MPa. However, the compressive strength of the specimens bonded by alkali-activated cement continues to increase from 6.47 MPa to 7.17 MPa after curing 14 days and 28 days, and at 28 days are only slightly less than the strengths of the sulphoaluminate specimens. Under the same conditions (the same curing environment and curing age), there may be more hydration reaction and hydration products (such as ettringite and gel) forming a denser microstructure for sulphoaluminate specimens [34]. Therefore, the compressive strength of the B2 specimens is the best in Figure 4.

When the water-to-binder ratio is 3, the compressive strengths of all the specimens bonded by ordinary Portland cement and sulphoaluminate cement are more than 2 MPa and less than 3 MPa, as shown in Figure 5. Only the compressive strengths of the specimens bonded by alkali-activated cement are close to 4 MPa (3.97 MPa) after curing for 28 days. The compressive strengths of all the specimens when the water-to-binder ratio is 3 are lower than those of the specimens when the water-to-binder ratio is 2. It shows that the increased water-to-binder ratio has a great influence on the compressive strength of the specimens bonded with the several cementing binders. On the one hand, it could form calcium silicate hydrates gel for the reaction between silicate anions of the tailing and calcium cations of

lime, which was very critical for cementitious properties of the alkali-activated cement [14]. The reactions of the calcium silicate hydrate gel, CaCO_3 , and ettringite would become more and more during curing in the water for the alkali-activated cement [14,33,34]. Thus, the compressive strengths of the F3 specimens are more than that of the A3 and B3 specimens in Figure 5.

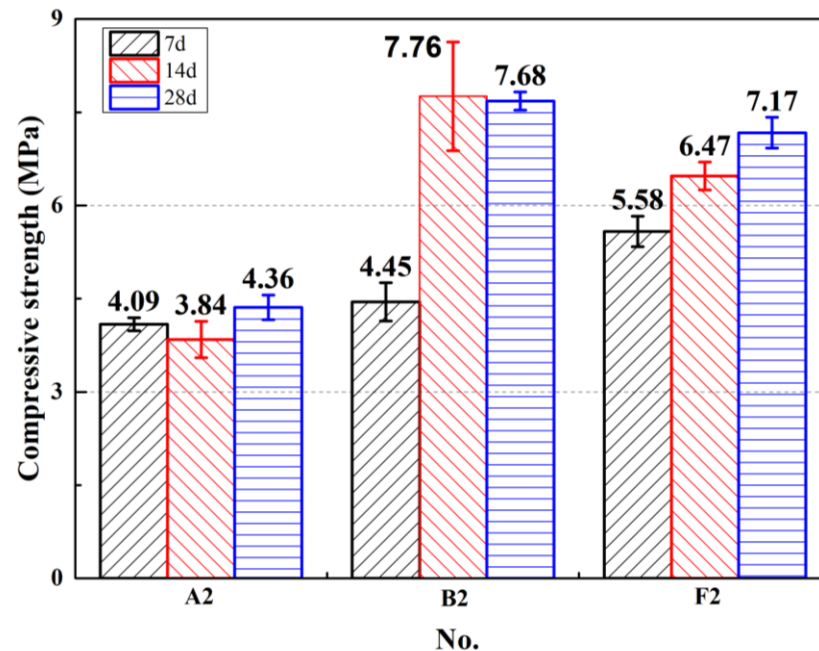


Figure 4. Compressive strength of specimens when water-to-binder ratio is 2.

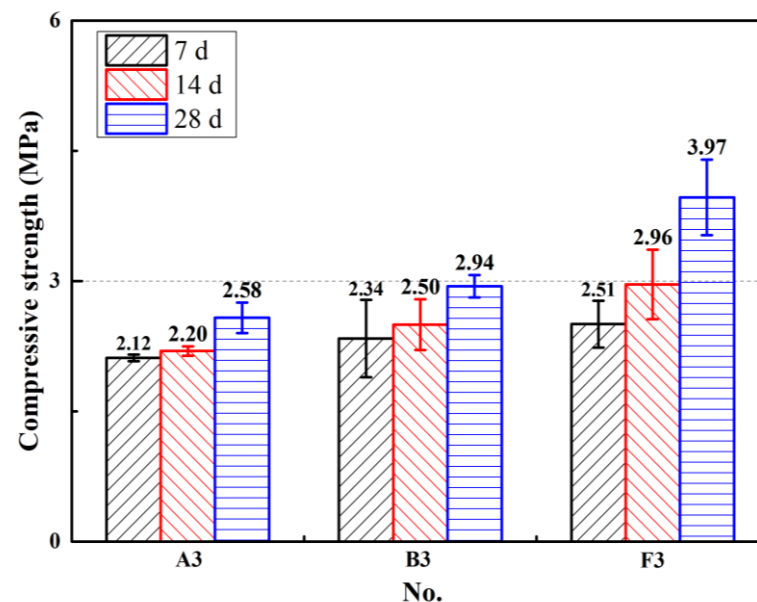


Figure 5. Compressive strength of specimens when water-to-binder ratio is 3.

The compressive strengths of the specimens bonded by ordinary Portland cement and sulphoaluminate cement are all more than 1 MPa and less than 2 MPa when the water-to-binder ratio increases to 4, as shown in Figure 6. However, the compressive strengths of the specimens bonded by alkali-activated cement are more than 3 MPa (3.02 MPa) after 28 days.

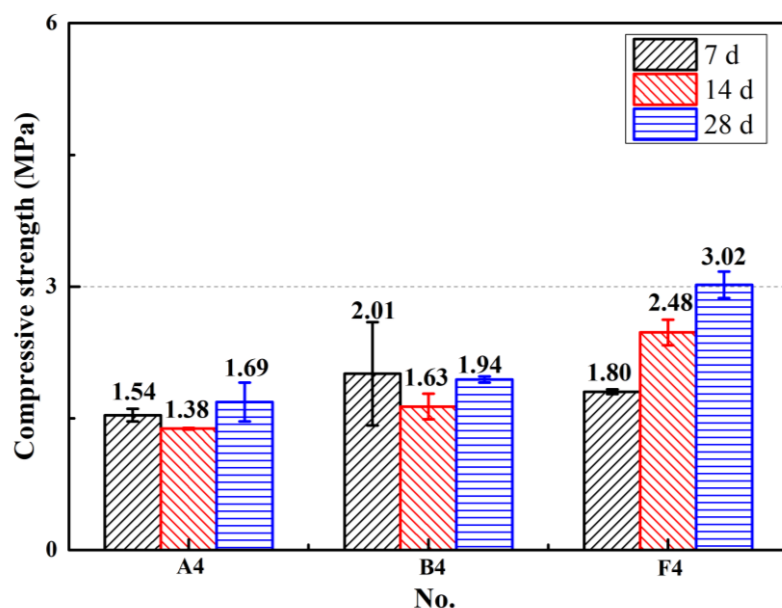


Figure 6. Compressive strength of specimens when water-to-binder ratio is 4.

According to the above results, for the water-to-binder ratio of 3 and 4, the compressive strength of the specimens bonded by ordinary Portland cement and sulphoaluminate cement are all lower 3 MPa. The compressive strength of the specimens bonded by ordinary Portland cement is the lowest with the water-to-binder ratio ranged from 2 to 4. The compressive strengths of the specimens bonded by alkali-activated cement are all more than 3 MPa after 28 days, thus indicating that the strength of the specimens bonded by alkali-activated cement increases steadily with the increasing curing age and even with a larger water-to-binder ratio.

For the curing of 7 days (in the laboratory air) and 28 days (curing 7 days in the laboratory air first and then curing 21 days in water), when the water-to-binder ratio increases from 2 to 4, the compressive strength of the specimens bonded by ordinary Portland cement increased only 6.6% (the water-to-binder ratio is 2) to 21.7% (the water to binder is 3), and the compressive strength of the specimens bonded by sulphoaluminate cement changed from -12.0% (decrease) to 72.6% (the water-to-binder ratio is 2). However, the compressive strength of the specimens bonded by alkali-activated cement all increased 28.5% (the water-to-binder ratio is 2) to 67.8% (the water-to-binder ratio is 4). The limestone powder and quicklime, which are only in the alkali-activated cement, can form calcium silicate hydrate gel, CaCO_3 , and ettringite and improve the compressive strength [14,33,34]. Therefore, only the compressive strength of the specimens bonded by alkali-activated cement increases with increasing curing age.

3.2. Microstructure Characterization of Tailings Consolidation Samples

The differences in the compressive strengths of the several specimens bonded by various binders may be due to the different microstructure characteristics. In order to find the differences in the microstructure characteristics of full tailings' cementing-material samples with various binders, XRD, SEM, and MIP tests were executed, and the results are shown in Figure 7, Figure 8, and Figure 9, respectively.

3.2.1. XRD Analysis

The XRD results are shown in Figure 7; according to the XRD patterns, there are SiO_2 , CaCO_3 , $\text{Ca}_3\text{Fe}_2(\text{SiO}_4)_3$, and ettringite (Aft) in the samples bonded by three kinds of binders. Some compounds, SiO_2 , CaCO_3 , and $\text{Ca}_3\text{Fe}_2(\text{SiO}_4)_3$, are from the raw material, tungsten ore tailings (Figure 2). Some of the CaCO_3 may come from the raw material limestone powder directly and the hydration products of the raw material of quicklime powder indirectly for

the binder alkali-activated cement in Figure 7. The remaining CaCO_3 is mainly from the hydration products of the binder, because only alkali-activated cement includes the above two kinds of compositions (limestone powder and quicklime powder) [33,34]. Meanwhile, the AFt diffraction peaks are different among the various full tailings' cementing samples in Figure 7. There is more AFt in the sample of F3 than that of F4, and there is more AFt in the sample of B3 than that of A3, according to the XRD test results shown in Figure 7. For this reason, the compressive strength of the specimens bonded by alkali-activated cement with the water-to-binder ratio of 3 is higher than that with a water-to-binder ratio of 4, and the compressive strength of the specimens bonded by the sulphoaluminate cement is higher than that of ordinary Portland cement at the same water-to-binder ratio, as shown in Figure 6. In addition, some gel products (C-S-H) were generated in the tailings' consolidation samples, but there are no relevant diffraction peaks in Figure 7, due to fact that the cementing-agent-to-tailings-weight ratio is less than 0.15 and much too little in Table 2.

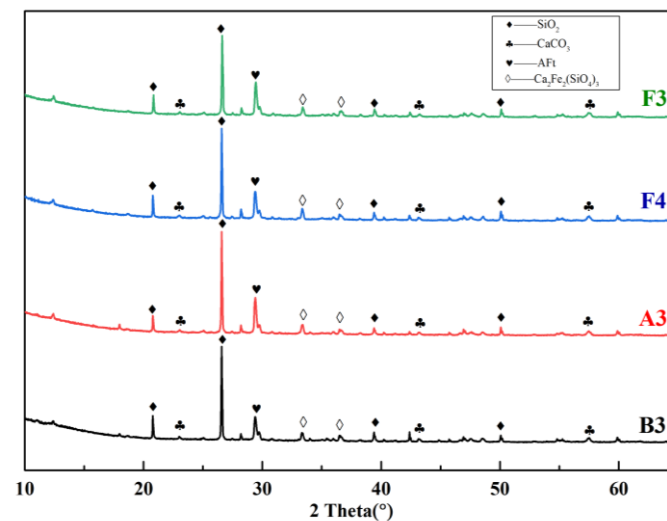


Figure 7. XRD patterns of the different samples.

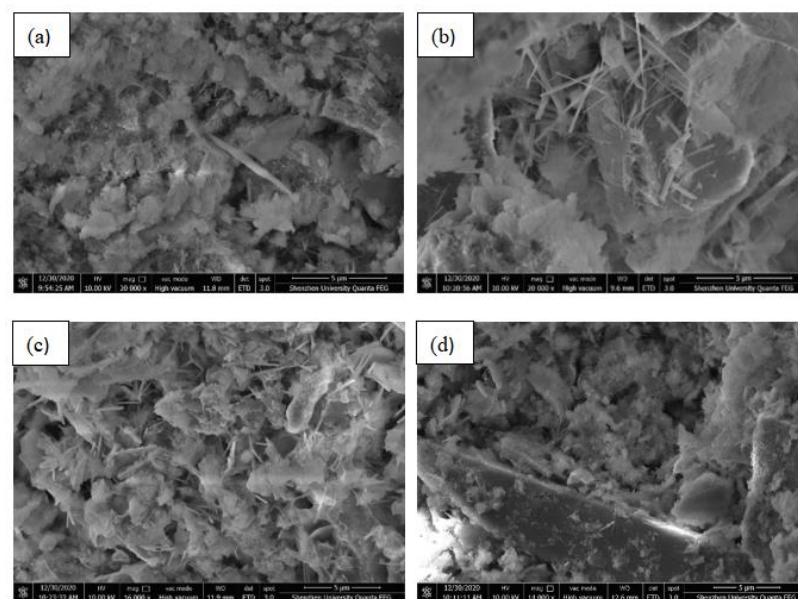


Figure 8. SEM images of samples with three binders. (a–d) are A3, B3, F3 and F4 after curing 28 days, respectively.

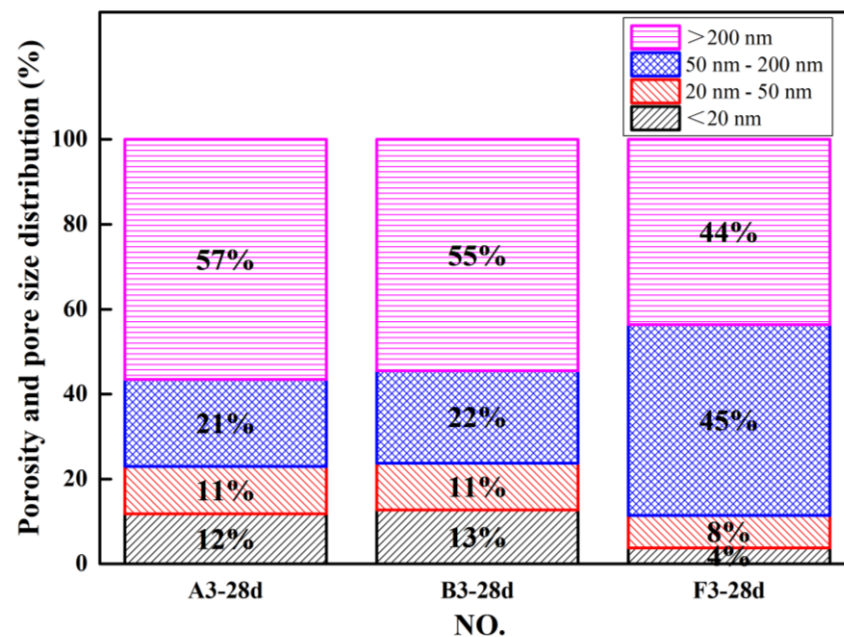


Figure 9. Pore structure of some samples with different cement agents.

3.2.2. SEM Analysis

To observe the micromorphology of the specimens after compressive-strength tests, some samples were tested by SEM after 28 days. The results are shown in Figure 8.

Obviously, there are still many solid particles in the samples in Figure 8, which are mainly tailing particles of tungsten ore. Furthermore, it can be seen that there are obvious needlelike crystals in Figure 8 which are mainly AFt crystals produced by hydration reaction of the binder with water [33,34]. Nevertheless, there are more AFt crystals in the samples with sulphoaluminate cement (B3 in Figure 8b) than in those of ordinary Portland cement (A3 in Figure 8a), and there are more AFt crystals in the samples with the water-to-binder ratio of 3 (F3 in Figure 8c) than in those with the water-to-binder ratio of 4 (F4 in Figure 8d). These results are the same as the results of the XRD testing reported in Section 3.2.1. Simultaneously, the microstructure of B3 is denser than that of A3 after 28 days, and the microstructure of F3 is denser than that of F4 after curing 28 days, as shown in Figure 8. The denser that the microstructure is, the higher the compressive strength is. Hence, the compressive strength of B3 is higher than that of A3 after 28 days, and the compressive strength of F3 is higher than that of F4 after curing 28 days.

3.2.3. MIP Analysis

In order to understand the pores' structure, some samples with various cementing agents and various water-to-binder ratio were tested by the MIP method. The porosities of the A3, B3, and F3 samples are all about 42%, and the results of the porosity and pore size distribution are shown in Figure 9. The ratio of the >200 nm pore of A3, B3, and F3 is 57%, 55%, and 44%, respectively. The smaller the >200 nm pore is, the denser the microstructure is and the higher the compressive strength of the specimens is. Therefore, the compressive strength of the F3 sample is higher than that of the B3 and A3 samples in Figure 5.

Figure 9 shows that the pore distribution is mainly in the range larger than 200 nm. The porosity and pore size distribution of A3 are very close to those of B3; the difference of the ratio of pore size distribution between A3 and B3 is just about 2%. However, the porosity and pore size distribution of F3 differs greatly from that of A3 and B3; in particular, there are smaller >200 nm pores and much larger 50–200 nm pores in F3 than in A3 and B3. This shows that alkali-activated cement reacts gradually after consolidating, making the structure with smaller >200 nm pores and larger 50–200 nm pores more compact, and the compressive strength gradually improved.

Figure 9 shows that the pore sizes are primarily larger than 50 nm, that there are many internal pores (>200 nm pore) in the sample, and that the proportion of the macropores (>50 nm pore) is relatively large (more than 77%). The material belongs to high-water material, and the porous structure is conducive to the material absorbing water, which can better solidify the tailings with large water content. Because the solidified tailings are used for mine filling, the strength requirement of the material is not very high. The compressive test shows that the strength of the material can reach 3 MPa. Solidified filling materials with such strength are sufficient for most engineering applications [33]. According to current research, compared with the other two binders, the alkali-activated cement has a higher strength in the case of a large water–binder ratio, so it has better application prospects [14,17,33,34].

3.3. Environmental Impact Analysis

The environmental impact of alkali-activated cement, Portland cement, and sulphoaluminate cement as binders of tungsten tailings was quantitatively analyzed by comparing their energy consumption and pollutant emissions during production and transportation. Portland cement and sulphoaluminate cement need to be fired at a high temperature in the factory before they are used, so this study should include the production and transportation of Portland cement, sulphoaluminate cement and alkali-activated cement, as well as the preparation process of materials [33,35].

The basic data needed primarily include the energy input to the research object at each stage within the scope boundary and the emissions of harmful substances to the environment, such as CO and CO₂ [29]. The review of the literature and the laboratory research enumerate and describe the steps and processes involved in the entire process, from raw material preparation to tungsten tailing consolidation. The basic data of the several materials involved in this study are from the literature references and from a Chinese commercial database (named eBalance). In order to facilitate the follow-up study, the assumptions are listed as follows. It is assumed that the average transportation distance of tungsten tailings from the acquisition site to the treatment laboratory is 1 km, and the transportation distance from the purchase or mining source of cement materials and alkali-activated cement to the laboratory is 1 km.

Assuming that the transportation unit price of various materials used in the study is the same, the environmental impact of various materials in the entire transportation process is the same, so the inventory file of environmental transportation is not listed in the life cycle evaluation in Table 3. The functional units of this evaluation are all 1 cubic meter of tailings consolidation material in Table 3. The cement's basic data in the database include the process of material mining, production, and preparation, so we can search and apply them directly from the database. Considering that this study is only in laboratory research, some data are difficult to obtain at present or difficult to obtain under some complex situations, so this paper does not include the analysis and evaluation of environmental indicators involved in the whole stage of new material production and transportation application and demolition. The basic inventory data of Portland cement, Sulphoaluminate cement, and Alkali-activated cement are shown in Table 3. These basic inventory data include primary energy consumption and harmful gas (CO₂, CO, C_xH_y, NO_x, and SO₂) emissions, as shown in Table 3.

Table 3. Basic inventory data.

Material/Consumption Data	Primary Energy Consumption (PEC)/MJ	CO ₂ /kg	CO/kg	C _x H _y /kg	NO _x /kg	SO ₂ /kg
Portland cement/kg	4.500	0.890	1.80×10^{-3}	1.45×10^{-7}	4.10×10^{-3}	3.58×10^{-3}
Sulphoaluminate cement/kg	3.190	0.202	4.26×10^{-6}	3.91×10^{-8}	5.67×10^{-4}	1.31×10^{-4}

Table 3. Cont.

Material/Consumption Data		Primary Energy Consumption (PEC)/MJ	CO ₂ /kg	CO/kg	C _x H _y /kg	NO _x /kg	SO ₂ /kg
Alkali-activated cement	Mineral powder/kg (60%)	−1.600	−0.476	−9.61 × 10 ^{−4}	−7.77 × 10 ^{−8}	−8.41 × 10 ^{−4}	−3.56 × 10 ^{−4}
	Limestone/kg (15%)	0.246	0.010	1.33 × 10 ^{−5}	5.33 × 10 ^{−8}	1.70 × 10 ^{−5}	1.35 × 10 ^{−5}
	Quick lime/kg (4%)	5.413	1.192	1.40 × 10 ^{−4}	1.36 × 10 ^{−6}	3.68 × 10 ^{−4}	9.08 × 10 ^{−5}
	Gypsum/kg (10%)	1.618	0.102	1.16 × 10 ^{−4}	2.89 × 10 ^{−8}	2.60 × 10 ^{−4}	1.06 × 10 ^{−4}
	Sodium sulphate/kg (1%)	5.011	0.883	1.86 × 10 ^{−5}	1.71 × 10 ^{−7}	2.48 × 10 ^{−3}	4.37 × 10 ^{−4}
	Sulphoaluminate cement/kg (10%)	3.190	0.202	4.26 × 10 ^{−6}	3.91 × 10 ^{−8}	5.67 × 10 ^{−4}	1.31 × 10 ^{−4}
	Total alkali-activated cement/kg	−0.176	−0.197	−5.57 × 10 ^{−4}	−2.43 × 10 ^{−8}	−3.80 × 10 ^{−4}	−1.80 × 10 ^{−4}

Note: The primary energy consumption (PEC; the unit is MJ) data summarize various one-time energy consumptions, such as power (water power for electricity generation, wind power for electricity generation, solar energy for heat and power generation, and geothermal energy for heat and power generation), oil consumption, coal consumption, and so on [36]. Most of these data can be found in the eBalance database, so these data are directly used in this study instead of listing the specific consumption of power, oil consumption, and coal consumption individually.

The strength of the A2, B2, and F3 specimens just reaches 3 MPa, so this section only studies these specimens. The prepared specimen size is 40 mm × 40 mm × 40 mm in the present study, and the volume is 0.000064 m³. If 24 specimens can be prepared at one time, to prepare a specimen of 1 m³, the formula for calculating the mass of material required by the specimen is as follows:

$$M_i = m_i \frac{1}{0.000064 \times 24} \quad (1)$$

where M_i is the mass of 1 m³ binder required for the specimen, m_i is the mass of binder in the current test mix, and the unit is kg. The specific values are set forth in Table 4.

Table 4. Materials required for 1 m³ specimen.

Material	A2	B2	F3
Portland cement/kg	285.74	-	-
Sulphoaluminate cement/kg	-	285.74	-
Mineral powder/kg	-	-	114.30
Limestone/kg	-	-	28.57
Quick lime/kg	-	-	7.62
Gypsum/kg	-	-	19.05
Sodium sulphate/kg	-	-	1.90
Sulphoaluminate cement/kg	-	-	19.05
Total alkali-activated cement/kg	-	-	190.49

Carrying out the summary LCA calculation according to the described procedures provides the results summarized in Table 5. The primary energy consumption and harmful gas emission of A2 are much more than those of B2 in Table 5. Furthermore, F3 could save about 33.56 MJ primary energy consumption. Meanwhile, F3 also can cut down on harmful gas emissions, especially the CO₂ emissions.

The above inventory analysis summarizes the basic data of material consumption and emission indicators of each functional unit, but these independent indicators cannot directly reflect the impact of materials on the environment, so an environmental-impact assessment is needed. At present, SETAC divides the environmental impacts of LCA into global warming (greenhouse gas emissions), acidification, eutrophication, energy consumption, and human-health damage, as shown in Table 6.

Table 5. LCA data summary of 1 m³ specimen.

No.	Primary Energy Consumption (PEC)/MJ	CO ₂ /kg	CO/kg	C _x H _y /kg	NO _x /kg	SO ₂ /kg
A2	1285.84	254.31	0.51	4.14×10^{-5}	1.17	1.02
B2	911.51	57.72	1.22×10^{-3}	1.12×10^{-5}	0.16	0.04
F3	−33.56	−37.57	−0.11	-4.63×10^{-6}	-7.24×10^{-2}	-3.43×10^{-2}

Note: The primary energy consumption (PEC; the unit is MJ) data summarize various one-time energy consumptions, such as power (water power for electricity generation, wind power for electricity generation, solar energy for heat and power generation, and geothermal energy for heat and power generation), oil consumption, coal consumption, and so on [36]. Most of these data can be found in the eBalance database, so these data are directly used in this study instead of listing the specific consumption of power, oil consumption, and coal consumption individually.

Table 6. Environmental-impact classification and equivalent number.

Types of Environmental Impacts	Environmental-Impact Factors	Reference Object	Impact Potential Unit	Equivalence Factor
Global warming potential (GWP)	CO ₂	CO ₂	kg CO ₂ eq./kg	1
	NO _x			3.20
	CO			25
	C _x H _y			2
Acidification (AP)	NO _x	SO ₂	kg SO ₂ eq./kg	0.7
	SO ₂			1
Nitridation (NP)	NO _x	NO _x	kg NO _x eq./kg	0.013
	CO			0.012
Human health damage (HCA)	NO _x	human body	kg human body eq./kg	0.78
	SO ₂			1.2

The data about environmental pollution impact of a 1 m³ specimen are listed in Table 7.

Table 7. Environmental-pollution impact of a 1 m³ specimen.

Types of Environmental Impacts	PEC (MJ)	GWP (kg)	AP (kg)	NP (kg)	HCA (kg)
A2	1285.83	270.80	1.839	0.015	2.143
B2	911.51	58.26	0.152	0.002	0.173
F3	−33.56	−40.55	−0.085	-9.41×10^{-4}	−0.10

Note: Table column abbreviations are as described below.

Primary energy consumption (PEC, the unit is MJ): The PEC data summarize various one-time energy consumptions, such as power (water power for electricity generation, wind power for electricity generation, solar energy for heat and power generation, and geothermal energy for heat and power generation), oil consumption, coal consumption, and so on [36]. Most of these data can be found in the eBalance database, so these data are directly used in this study instead of listing the specific consumption of power, oil consumption, and coal consumption individually.

Global warming potential (GWP; the unit is kg): Taking CO₂ as the reference gas, the global warming potential is an index that expresses the greenhouse effect caused by greenhouse gases dominated by CO₂. It is used in the life cycle assessment to characterize the impact of materials on the environmental greenhouse effect. There are more than 30 kinds of gases that cause the greenhouse effect, among which CO₂, CO, NO_x, and C_xH_y have significant effects.

Acidification potential (AP; the unit is kg): Acidification refers to the pollution of the atmosphere that leads to the acidification of rainwater into acid rain, and the acidification of soil and water sources after falling on the surface, resulting in the decline of their functions, which will have a serious impact on the environment and human life. According to the current research findings, the main substances causing acidification are SO₂, NO_x, etc.

Eutrophication (NP; the unit is kg): Eutrophication is mainly caused by water pollution caused by excessive nitrogen, phosphorus, and other elements. The main factor causing this problem is excessive NO_x emissions.

Human health damage (HCA; the unit is kg): This index quantifies the overall emission of substances harmful to the human body and can express the impact of materials on human life and production. The factors harmful to human beings mainly include CO , SO_2 , NO_x , etc.

Table 7 shows that the preparation of alkali-activated cement sand consolidation specimen has the least impact on the environment in terms of energy input and greenhouse gas emissions. Compared with the A2 and B2 specimens, the PEC values of the F3 specimen are reduced by 1319.32 MJ and 945 kg, respectively; the GWP decreased by 311.35 kg and 98.81 kg, respectively. The values of AP, NP, and HCA were lower than those of other categories, indicating that the direct effects of this material on environmental acidification, eutrophication, and human body damage were not very significant.

The life-cycle-assessment analysis's result of alkali-activated cement is negative, so the environmental impact performance of the specimen has a positive benefit. This is mainly because the tungsten tailing originally belonged to the solid waste produced in tungsten ore smelting, and separate treatment will cause environmental pollution and economic expenditure. In this study, the alkali-activated cement took the tungsten ore powder as one of the main raw materials; collecting the ore powder for recycling utilization can avoid the environmental pressure caused by the direct discharge of the ore tailing, thus providing an effective method for the recovery and treatment of ore tailing. Compared with Portland cement and sulphoaluminate cement, alkali-activated cement provides significant advantages in relation to environmental protection, having a positive impact for environmental protection and effectively reducing the cost of mine filling, as using alkali-activated slag as a binder for the full tailing filling material has positive benefits for the environmental and economic aspects of mine-filling work.

4. Conclusions

In this study, ordinary Portland cement, sulphoaluminate cement, and alkali-activated cement were used as binders to prepare full-tailings high-water materials for filling with various water-to-binder ratios. The compressive-strength development of consolidated tungsten tailings prepared with various binders was observed, and the influence of various water-to-binder ratios on the strength development was analyzed. Based on the life cycle theory, the environmental impact assessment and comparison of mine backfill materials prepared by various curing agents were carried out. The following conclusions were reached:

- (1) The compressive strength can reach 3 MPa when the water-to-binder ratio is 2 or below 2, while only the alkali-activated cement can make the compressive strength still reach 3 MPa when the water-to-binder ratio is 3
- (2) The hydration reaction of the three binders produces gel and ettringite, which can form a cementitious microstructure. The larger pore size (>200 nm) is much smaller in the samples of the alkali-activated-cement-solidified tailings than those of Portland cement and sulphoaluminate cement.
- (3) The environmental load of the alkali-activated cement is significantly lower than that of Portland cement and sulphoaluminate cement. Compared with the A2 and B2 specimens, the primary energy consumption values of the F3 specimens are reduced by 1319.32 MJ and 945 kg, respectively. Moreover, the GWP decreased by 311.35 kg and 98.81 kg, respectively.
- (4) The quantitative LCA shows that the environmental protection pressure of slag powder is reduced sufficiently, and the impact of alkali-activated cement for sand consolidation is positive.

Author Contributions: Data curation, P.L.; Formal analysis, Z.D. and P.C.; Funding Acquisition, C.H.; Investigation, P.L.; Methodology, Z.D. and C.H.; Writing-original draft, P.L.; Writing-review & editing, Z.D. and P.C. All authors have read and agreed to the published version of the manuscript.

Funding: This research was funded by [National Natural Science Foundation of China] grant number [41602352].

Data Availability Statement: Not applicable.

Conflicts of Interest: The authors declare no conflict of interest.

References

1. Lutandula, M.S.; Maloba, B. Recovery of cobalt and copper through reprocessing of tailings from flotation of oxidised ores. *J. Environ. Chem. Eng.* **2013**, *1*, 1085–1090. [\[CrossRef\]](#)
2. Lazorenko, G.; Kasprzhitskii, A.; Shaikh, F.; Krishna, R.; Mishra, J. Utilization potential of mine tailings in geopolymers: Physicochemical and environmental aspects. *Process. Saf. Environ. Prot.* **2021**, *147*, 559–577. [\[CrossRef\]](#)
3. Mansour, E.; Thomas, B.; Emmanuel, M.; Dee, B.; Daniel, M.F.; Chris, J.M. Designing mine tailings for better environmental, social and economic outcomes: A review of alternative approaches. *J. Clean. Prod.* **2014**, *84*, 411–420.
4. Liu, L.; Hao, Q.; Hao, Z.; Zhang, J.; Fei, H. Current Status of the Comprehensive Utilization of Metallic Mine Tailings in China. *Geol. Prospect.* **2013**, *49*, 437–443. (In Chinese)
5. Nan, Z.; Erbao, D.; Meng, L.; Jixiong, Z.; Chaowei, D. Determination of the stability of residual pillars in a room-and-pillar mining goaf under eccentric load. *Energy Rep.* **2021**, *7*, 9122–9132.
6. Peng, J.; Zhou, M.F.; Hu, R.; Shen, N.; Yuan, S.; Bi, X.; Du, A.; Qu, W. Precise molybdenite Re-Os and mica Ar-Ar dating of the Mesozoic Yaogangxian tungsten deposit, central Nanling district, South China. *Miner. Depos.* **2006**, *41*, 661–669. [\[CrossRef\]](#)
7. Feng, C.; Zeng, Z.; Zhang, D.; Qu, W.; Du, A.; Li, D.; She, H. SHRIMP zircon U-Pb and molybdenite Re-Os isotopic dating of the tungsten deposits in the Tianmenshan-Hongtaoling W-Sn orefield, southern Jiangxi Province, China, and geological implications. *Ore Geol. Rev.* **2011**, *43*, 8–25. [\[CrossRef\]](#)
8. Liu, H.; Liu, H.L.; Nie, C.X.; Zhang, J.X.; Steenari, B.M.; Ekberg, C. Comprehensive treatments of tungsten slags in China: A critical review. *J. Environ. Manag.* **2020**, *270*, 110927. [\[CrossRef\]](#)
9. Sheng, J.F.; Liu, L.J.; Wang, D.H.; Chen, Z.H.; Ying, L.J.; Huang, F.; Wang, J.H.; Zeng, L. A preliminary review of metallogenic regularity of tungsten deposits in China. *Acta Geol. Sin.-Engl.* **2015**, *89*, 1359–1374.
10. Dai, Y.Y. Study on the New Cleaner Process of Comprehensive Recovery of Valuable Metals from Tungsten Slags. Ph.D. Thesis, Central South University, Changsha, China, 2013. (In Chinese)
11. Alfonso, P.; Castro, D.; Garcia-Valles, M.; Tarragó, M.; Tomasa, O.; Martínez, S. Recycling of tailings from the Barruecopardo tungsten deposit for the production of glass. *J. Therm. Anal. Calorim.* **2016**, *125*, 681–687. [\[CrossRef\]](#)
12. Alfonso, P.; Tomasa, O.; Garcia-Valles, M.; Tarragó, M.; Martínez, S.; Esteves, H. Potential of tungsten tailings as glass raw materials. *Mater. Lett.* **2018**, *228*, 456–458. [\[CrossRef\]](#)
13. Alfonso, P.; Tomasa, O.; Garcia-Valles, M.; Tarrago, M.; Martínez, S. Glass-ceramic crystallization from tailings of the Morille tungsten deposit, Spain. *Mater. Lett.* **2022**, *312*, 131694. [\[CrossRef\]](#)
14. Peng, K.; Yang, H.M.; Ouyang, J. Tungsten tailing powders activated for use as cementitious material. *Powder Technol.* **2015**, *286*, 678–683. [\[CrossRef\]](#)
15. Liu, W.Z.; Wu, T.; Li, Z.; Hao, X.J.; Lu, A.X. Preparation and characterization of ceramic substrate from tungsten mine tailings. *Constr. Build. Mater.* **2015**, *77*, 139–144. [\[CrossRef\]](#)
16. Zhu, Y.; Guo, B.; Zuo, W.R.; Jiang, K.X.; Chen, H.H.; Ku, J.G. Effect of sintering temperature on structure and properties of porous ceramics from tungsten ore tailings. *Mater. Chem. Phys.* **2022**, *287*, 126315. [\[CrossRef\]](#)
17. Pacheco-Torgal, F.; Castro-Gomes, J.P.; Jalali, S. Investigations of tungsten mine waste geopolymeric binder: Strength and microstructure. *Constr. Build. Mater.* **2008**, *22*, 2212–2219. [\[CrossRef\]](#)
18. Pacheco-Torgal, F.; Castro-Gomes, J.P.; Jalali, S. Tungsten mine waste geopolymeric binder: Preliminary hydration products investigations. *Constr. Build. Mater.* **2009**, *23*, 200–209. [\[CrossRef\]](#)
19. Jiawei, L.; Wanghua, S.; Dingyang, Z.; Qingjie, Z. Durability of water-affected paste backfill material and its clean use in coal mining. *J. Clean. Prod.* **2020**, *250*, 119576.
20. Huang, Y.C.; Sun, H.H. Study on mechanical properties of high water consolidation tailings filling material. *Met. Mine* **1997**, *249*, 13–15+40. (In Chinese)
21. Behera, S.K.; Ghosh, C.N.; Mishra, D.P.; Singh, P.; Mishra, K.; Buragohain, J.; Mandal, P.K. Strength development and microstructural investigation of lead-zinc mill tailings based paste backfill with fly ash as alternative binder. *Cem. Concr. Comp.* **2020**, *109*, 103553. [\[CrossRef\]](#)
22. Bin, T. High Percentage of Water Rapid Solidifying Material and Tailings for Cementing Filling. *Ind. Min. Process.* **1999**, *2*, 15–16. (In Chinese)
23. Ahmadi, S.; Ghasemzadeh, H.; Changizi, F. Effects of A low-carbon emission additive on mechanical properties of fine-grained soil under freeze-thaw cycles. *J. Clean. Prod.* **2021**, *304*, 127157. [\[CrossRef\]](#)

24. Changizi, F.; Ghasemzadeh, H.; Ahmadi, S. Evaluation of strength properties of clay treated by nano-SiO₂ subjected to freeze–thaw cycles. *Road Mater. Pavement Des.* **2022**, *23*, 1221–1238. [[CrossRef](#)]
25. Li, C.; Jin, J.; Wu, P.; Xu, B. Effect of Freeze–Thaw Cycles on Shear Strength of Tailings and Prediction by Grey Model. *Minerals* **2022**, *12*, 1125. [[CrossRef](#)]
26. Ahmadi, S.; Ghasemzadeh, H.; Changizi, F. Effects of thermal cycles on microstructural and functional properties of nano treated clayey soil. *Eng. Geol.* **2021**, *280*, 105929. [[CrossRef](#)]
27. Ye, S.; Guangcheng, L.; Cong, M.; Youjun, X.; Jionghuang, H. Design and preparation of Ultra-High Performance Concrete with low environmental impact. *J. Clean. Prod.* **2019**, *214*, 633–643.
28. Cabeza, L.F.; Rincón, L.; Vilariño, V.; Pérez, G.; Castell, A. Life cycle assessment (LCA) and life cycle energy analysis (LCEA) of buildings and the building sector: A review. *Renew. Sustain. Energy Rev.* **2014**, *29*, 394–416. [[CrossRef](#)]
29. Huang, H.; Wang, T.; Kolosz, B.; Andresen, J.; Garcia, S.; Fang, M.X.; Maroto-Valer, M.M. Life-cycle assessment of emerging CO₂ mineral carbonation-cured concrete blocks: Comparative analysis of CO₂ reduction potential and optimization of environmental impacts. *J. Clean. Prod.* **2019**, *241*, 118359. [[CrossRef](#)]
30. Cucurachia, S.; Giesena, C.D.; Guinée, J. Ex-ante LCA of emerging technologies. *Procedia CIRP* **2018**, *69*, 463–468. [[CrossRef](#)]
31. Matthias, B.; Amaryllis, A.; Pieter, B.; Katrien, B.; Steven, V.P. The Future of Ex-Ante LCA? Lessons Learned and Practical Recommendations. *Sustainability* **2019**, *11*, 5456.
32. Huang, Z.Q.; Zhang, S.Y.; Wang, H.L.; Liu, R.K.; Cheng, C.; Shuai, S.Y.; Hu, Y.J.; Zeng, Y.H.; Yu, X.Y.; He, G.C.; et al. Recovery of wolframite from tungsten mine tailings by the combination of shaking table and flotation with a novel “crab” structure sebacyl hydroxamic acid. *J. Environ. Manag.* **2021**, *317*, 115372. [[CrossRef](#)]
33. Cui, P.; Huang, W.; Yi, Q.; Zhu, D.; Hong, C.Y. Study on the concreted properties and mechanism of filling materials of tungsten whole tailings. *China Min. Mag.* **2020**, *29*, 108–115. (In Chinese)
34. Wang, J.F.; Ma, L.W.; Lu, L.L.; Fu, Q.L.; Li, X.L.; Zhang, R.S.; Liu, Y.W. Improving the wear resistance and chloride permeability of sulphoaluminate cement by spindle-like calcium carbonate modification. *Mater. Today Commun.* **2022**, *32*, 104037. [[CrossRef](#)]
35. Behera, S.K.; Mishra, D.P.; Singh, P.; Mishra, K.; Mandal, S.K.; Ghosh, C.N.; Kumar, R.; Mandal, P.K. Utilization of mill tailings, fly ash and slag as mine paste backfill material: Review and future perspective. *Constr. Build. Mater.* **2021**, *309*, 125120. [[CrossRef](#)]
36. Olkuski, T.; Suwała, W.; Wyrwa, A.; Zyśk, J.; Tora, B. Primary energy consumption in selected EU Countries compared to global trends. *Open Chem.* **2021**, *19*, 503–510. [[CrossRef](#)]

Disclaimer/Publisher’s Note: The statements, opinions and data contained in all publications are solely those of the individual author(s) and contributor(s) and not of MDPI and/or the editor(s). MDPI and/or the editor(s) disclaim responsibility for any injury to people or property resulting from any ideas, methods, instructions or products referred to in the content.